CFD-based reduced model for the simulation of thermocline Thermal Energy Storage systems

Alberto Pizzolato[a], Filippo Donato[b], Vittorio Verda[a], Massimo Santarelli[a]

Energy Department, Politecnico di Torino, Corso Duca degli Abbruzzi 24, 10129, Torino, Italy, +390110904478, alberto.pizzolato@polito.it,

[b] ENEA UTRINN Via Anguillarese 301, 00123 Rome, Italy

Abstract

Thermocline thermal storages are widely used in energy systems. Computational Fluid Dynamic (CFD) can be used for an accurate simulation of the physical phenomenon but its implementation in system-level annual simulations is hardly possible because of the huge computational time required. The present paper proposes a novel approach for the utilization of CFD simulation results in system-level annual simulations and optimizations. An analytical function able to represent the dimensionless vertical temperature profile inside the tank is parameterized statistically using the results of multiple simulations of a CFD model, which have been previously validated with experimental data. The *reduced* model obtained is then compared to other CFD simulations under highly variable conditions, showing a satisfactory degree of agreement (the mean absolute error and the error standard deviation are calculated to be 1.52 K and 1.93 K respectively). Furthermore, it is demonstrated that this approach can be conveniently adopted for the modeling of a wide range of systems with a single tank thermal energy storage, from Concentrated Solar Power to District Heating.

Highlights

- A CFD model is implemented and validated with experimental results.
- The logistic distribution is chosen as suitable function to represent the vertical temperature profile
- The function is statistically parameterized with multiple CFD simulations
- The function is successfully tested in many different conditions

Keywords: Model Reduction; Thermal Energy Storage; Thermocline Storage Simulation;

Nomenclature

Letters and abbreviations

T^*	Dimensionless temperature, $T^* = \frac{T-T_{mn}}{T_{mx}-T_{mn}}$ $[-]$
$\dot{V}$	Volumetric flow rate $\left[\frac{m^3}{s}\right]$
c_p	Specific Heat $\left[\frac{J}{kgK}\right]$
v_z	Velocity along axial direction $\left[\frac{m}{s}\right]$
z^*	Dimensionless tank axial coordinate $[-]$
A	Area $[m^2]$
CDF	Cumulative Distribution Function
CFD	Computational Fluid-Dynamics
CSP	Concentrated Solar Power
E	Volumetric energy density $\left[\frac{J}{m^3}\right]$
Ex	Volumetric exergy density $\left[\frac{J}{m^3}\right]$
F	Force $[N]$
Fo	Fourier Number $[-]$
L	Length $[m]$
Pe	Peclet Number $[-]$
Pr	Prandtl number $[-]$
Q	Volumetric flow rate $\left[\frac{m^3}{s}\right]$
S	Quasi-variance of the logistic CDF $[-]$
T	Temperature $[K]$
u	Velocity component $\left[\frac{m}{s}\right]$
α	Thermal diffusivity $\left[\frac{m^2}{s}\right]$
μ	Mean of the logistic CDF $[-]$

μ	Dynamic viscosity $[Pa\ s]$
ρ	Density $\left[\frac{kg}{m^3}\right]$

Subscripts

$disch$	Discharged fluid
fm	Fully mixed
id	Ideal
mx	Maximum
mn	Minimum
0	Reference
T	Turbulent

1 Introduction

The thermocline Thermal Energy Storage (TES) tank is an important component in many energy systems. Its implementation has been recently proposed also for Concentrated Solar Power (CSP) [1], because this concept has a high cost reduction potential compared to the double-tank option, the most widely spread solution in commercial CSP plants [2]. In the literature, there are three main modeling approaches for the design and analysis of this kind of components: analytical models, numerical models and empirical models. The present work aims at presenting a novel model approach to overcome the main drawbacks that affect the available models while simulating the operating conditions over a long period of time.

Existing analytical solutions require complex mathematical analysis and most of the time have limited applicability in common problems. Yoo and Pak [6] found an analytical solution of the non-dimensional energy equation for two finite region in contact. The same authors showed that, if the Peclet number of the storage system considered is large enough (i.e. higher than 100), a simpler semi-infinite model can be used instead because the maximum temperature difference that is observed is less than 3 %. Under the semi-infinite approximation the problem is treated as a transient heat conduction with an interface moving at

constant velocity and the analytical solution of this type of problem was obtained by Eckert and Drake [7]. For the same range of Peclet number, a great agreement with the solution of Yoo and Pak was obtained by Chung [8] who proposed an integral approximation of the charging process of a stratified thermal storage tank .

Numerical approaches, instead, can provide very detailed insights and understanding of the physical phenomenon. Yaïci et al. [3], using a three-dimensional unsteady CFD model, investigated the influence of several design and operating parameters on the performance of a hot water storage tank during the charging process. On the other hand, Zavattoni et al. [5] used CFD for the understanding of the behavior of a rock-bed high temperature storage system during cyclic condition in order to investigate the temporal trend of the thermocline thickness.

Despite its enhanced accuracy, the CFD approach has the drawback of requiring a great use of computational resources. This represents an issue in the case of design/operation optimization problems. These problems involve multiple simulations often conducted over long periods (e.g. annual basis). In addition, the presence of a growing thermocline rises the need to adapt the plant control strategy in order to limit thermal diffusion and consequent mixing-related exergy destruction. Empirical models allow one to consider these aspects and make it possible to predict with sufficient accuracy the annual performance of the plant at the system level. Kolb [9] built a new TRNSYS component for the thermocline energy storage but the accuracy of his results is certainly influenced by the small number of control volumes adopted, i.e. 23. Angrisani et al. [10] used a similar approach: they have modeled the tank with 50 fully mixed equal volume nodes, for each of which uniform temperature is assumed. On the other hand, Roja and Bayon [11] suggested to use the cumulative logistic distribution to represent the vertical temperature profile in the tank and they proposed to parameterize the function using the results of a mono-dimensional laminar model. However, in their approach, turbulent effects are neglected. Furthermore, variation of the inlet temperature, of the mass flow rate and of the initial temperature are not considered.

2 The present work proposes a reduced model based on the logistic curve, which parameters have been obtained using the results of multiple turbulent simulations obtained from a CFD model. The CFD model has been validated using measured data of a real installation. The logistic function has been generalized in order to make it applicable to different operating conditions.Methodology

2.1 Numerical model

A CFD model has been built in order to reproduce the experimental results obtained at the PCS (Italian acronym standing for Prova Collettori Solari, i.e. Solar Collectors testing) facility present at the ENEA research center La Casaccia. The experimental system consists of a molten salts single-tank thermal energy storage with an integrated steam generator and has already been widely described in [1] and in [4]. The steam generator is submerged in the Heat Storage Medium. This component is a once-through countercurrent shell-and-tube heat exchanger with a helicoidal tube bundle: on the shell-side, in an annulus shaped channel, the molten salts flow downward thanks to naturally induced motion and, on the tube side, the water flows upward becoming superheated steam.

The computational domain adopted is graphically visible in Figure 1. Referring to the geometry depicted, the tank internal diameter D_{tank} is 1 m, while the height of the fluid free surface is placed at 2.1 m from the bottom. The internal cavity is the place where the steam generator is located and the geometry reproduces quite well the shape of the steam generator external envelope. From a careful examination of this shape, a Venturi tube is visible at the bottom; this device has the aim of slowing the fluid down during the discharge and avoid mixing enhancement. In the upper part, the steam generator external diameter D_{SG} is 0.125 m. It should be noted that the presented computational domain represents a simplification of the real geometry. In order to perform the simulation with a 2D grid, the integrated steam generator was moved in axial position, as proposed by Rivas et al. [4], while in the experimental facility it is placed at 0.5 m apart from the tank axis.

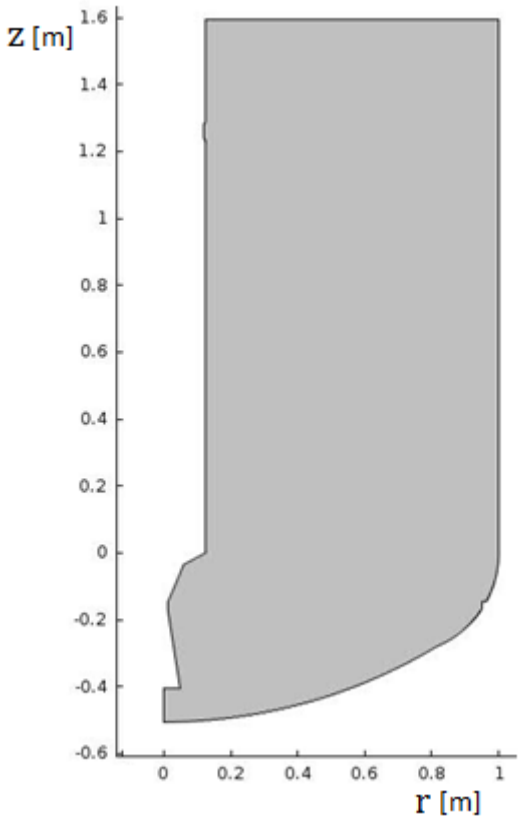

Figure 1. Geometry considered

Assuming negligible fluctuations in density, viscosity and thermal conductivity, the momentum, continuity and energy equations can then be written as follows:

$$\frac{\partial \rho}{\partial t} + \frac{\partial \rho u_j}{\partial x_j} = 0 \tag{1}$$

$$\frac{\partial \rho u_i}{\partial t} + \frac{\partial}{\partial x_j}\left(\rho\, u_j u_i\right) = -\frac{\partial P}{\partial x_i} + \frac{\partial \sigma_{ij}}{\partial x_j} + F_i \tag{2}$$

$$\frac{\partial \rho E}{\partial t} + \frac{\partial}{\partial x_j}\left(\rho u_j H\right) = \frac{\partial}{\partial x_j}\left(u_i \sigma_{ij}\right) - \frac{\partial}{\partial x_j}\left(\left(\frac{\mu}{PR} + \frac{\mu_T}{PR_t}\right)\left(\frac{\partial T}{\partial x_j}\right)\right) \tag{3}$$

Where:

- σ_{ij} is the tensor of viscous stresses defined as:
  $$\sigma_{ij} = 2(\mu + \mu_T)\left(S_{ij} - \frac{1}{3} S_{kk}\delta_{\mathrm{ij}}\right) \tag{4}$$

- S_{ij} is the tensor of shear stresses defined as:
  $$S_{ij} = \frac{1}{2}\left(\frac{\partial u_i}{\partial x_j} + \frac{\partial u_j}{\partial x_i}\right) \quad (5)$$
- H is the total enthalpy:
  $$H = E + \frac{P}{\rho} \quad (6)$$

For the closure of the equation set, a two-equation $k - \omega$ model has been implemented, which consists of solving for two variables: k, the turbulent kinetic energy, and omega, the specific rate of dissipation of kinetic energy.

The governing equations are converted to algebraic equations using the finite-elements technique in COMSOL. The discretization methods adopted were 2nd order Lagrange finite elements to model the velocity components and linear elements to model the pressure field. Time integration lies on a fully-implicit variable-order variable-time step BDF (Backward Differentiation Formula) scheme.

After a grid-independence study, a free-triangular mesh with 41331 elements has been chosen. The element size in the axial direction is 0.5 cm while in the radial direction is 1.5 cm.

The validation of the CFD model was an essential step of the methodology proposed in the framework of the present paper, allowing to proceed with multiple simulations in different conditions and to characterize the analytical function by statistical means. To obtain the data required for the experimental activities, the correct identification of the location of the measuring instruments is a crucial activity. For the validation of the model presented in this work, experimental data are taken from 14 thermocouples. The measuring devices are equally spaced every 10 cm on a long rod that is immersed vertically in the tank at r = 0.5 m. The rod is shorter than the tank (in fact it is only 1.3 m long) and, referring to Figure 1, the lower tip is placed at the height of $z = 0\ m$.

The validation of the discharging process is shown in Figure 2. Solid lines are the results obtained by the CFD simulation, while starred indicators are the experimental data. The mean absolute error is calculated to be 1.18 K with a standard deviation of 2.53 K.

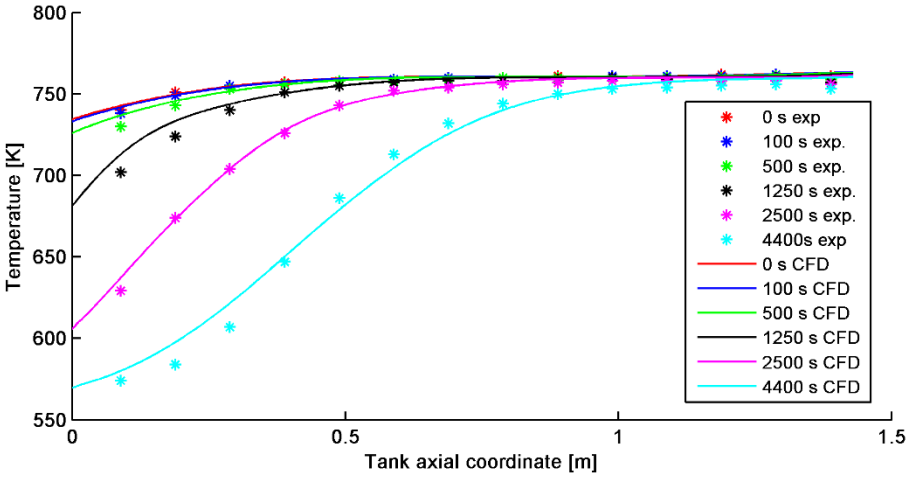

Figure 2. Validation of the discharging process

As far as the standby process is concerned, the results are compared for a total period of 100,000 seconds (approximately 27.8 hours). Referring to Figure 3, starred red indicators are the experimental results, while blue solid lines are obtained by the CFD simulation A very good agreement is reached in the upper part of the tank where the rate of temperature drop in time is perfectly predicted by the CFD mathematical and numerical model.

In both cases, the comparison with experimental data is considered to be satisfactory with a mean absolute error if 1.91 K and a standard deviation of 3.14 K. This means that the formulation of the physical problem is correct and that the numerical solutions obtained are able to reproduce the discharging and the standby process of the tank properly.

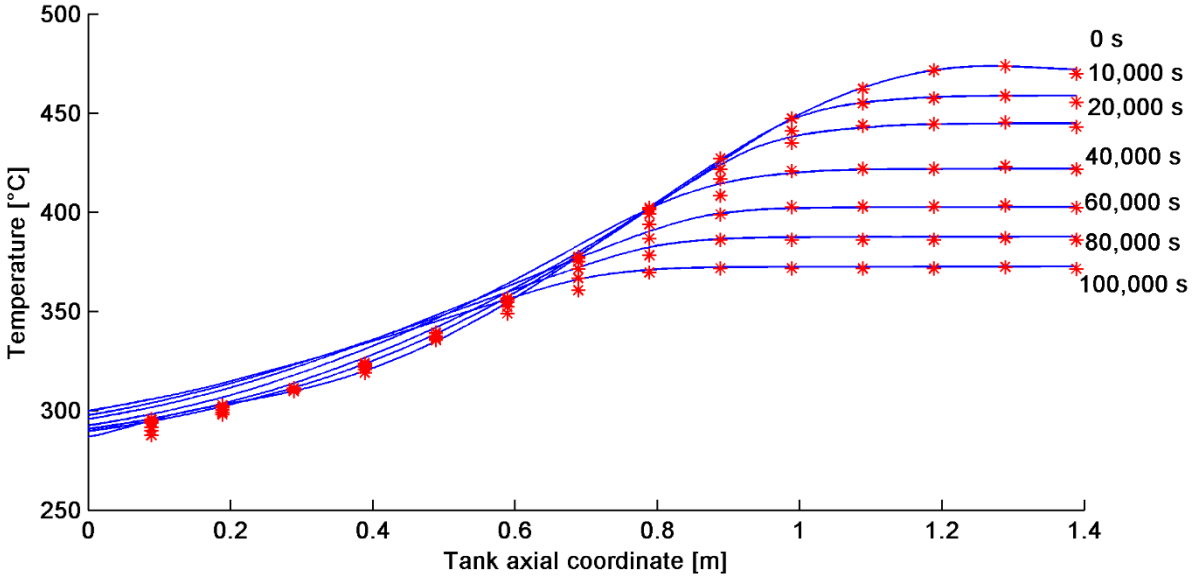

Figure 3. Validation of the standby process

2.2 Analytical function

The analysis of CFD simulation results, which is not reported here due to space constraints, shows that the isotherms are very flat during the normal operation of the tank and there are no appreciable temperature gradients in the radial direction. A one-dimensional approach can thus be very efficient in reproducing the storage tank performances. Furthermore, a non-dimensional approach is highly desirable for the optimization of the storage tank size where the dimensions of the tank, i.e. diameter and height, have to be varied continuously. Hence, the one-dimensional energy equation can be written conveniently in a non-dimensional form:

$$\frac{\partial T^*}{\partial Fo} = -Pe\frac{\partial T^*}{\partial z^*} + \frac{\partial^2 T^*}{\partial z^{*2}} \tag{7}$$

The dimensionless variables adopted are quite common in dimensional analysis of heat transfer problems [12]:

- The Fourier number, or dimensionless time: $Fo = \frac{\alpha t}{L^2}$
- The Peclet number, or dimensionless velocity: $Pe = Re\ Pr = \frac{v_z L}{\alpha}$
- The dimensionless axial coordinate: $z^* = \frac{z}{L}$

- The dimensionless temperaure: $T^* = \frac{(T-T_{mn})}{T_{mx}-T_{mn}}$

The tank temperature field of a vertical fluid column inside a thermal storage tank can be described by sigmoidal functions following the approach adopted by [11], [13] and [14]. In particular, the logistic CDF shows a great degree of agreement with experimental data obtained by molten salts storage tank operation for solar thermal power plants [11]. This statistic function is written in the form:

$$y(x;\ \mu, S) = y_{mn} + \frac{y_{mx}-y_{mn}}{1+e^{-\frac{x-\mu}{S}}} \tag{8}$$

The logistic distribution curve is used here for the parameterization of the thermocline dynamic processes. In fact, the numerical solution obtained with the CFD simulations are very similar to sigmoidal curves. If the mean value μ is substituted with the dimensionless thermocline center position z_c^*, we can adapt the parameterization of the function to the physical phenomenon. Following this approach, the dimensionless fluid temperature of a vertical column in the tank can be thus described at every instant of time with:

$$T^*(z^*, z_c^*, S) = \frac{1}{1+e^{-\frac{(z^*-z_c^*)}{S}}} \tag{9}$$

The other parameter, namely the statistical quasi-variance S, is a measure of the curve slope and has to be fitted statistically to the data obtained with multiple simulations in different conditions. However, a more convenient parameterization of the curve can be achieved utilizing the dimensionless thermocline thickness TC^*, which has a precise physical meaning. Due to the asymptotic behavior of the dimensionless temperature profile, the thermocline thickness depends on how much the maximum and minimum temperatures in the tank are approached and thus a minimum approach temperature difference should be fixed. This can be done by exploiting the statistical nature of the proposed function. In fact, in the logistic distribution, the tolerance interval can be expressed as:

$$z^* = \ z_c^* \pm \ nS \ln(2 + (3)^{0.5}) \tag{10}$$

In this way, it is possible to define the dimensionless thermocline thickness simply by fixing a conventional value of n. In formulas:

$$TC^* = 2nSln(2 + 3^{0.5}) \quad (11)$$

If n is set to 1.67, the thermocline thickness would consider 90 % of the total temperature gradient. By maintaining the value of n constant during the whole work, the thermocline thickness can be used directly for the parameterization of the logistic curve instead of S.

2.3 Statistical parameterization

Different simulations have been performed in order to get statistical insights on the variation of the TC^* parameter in many different conditions. Table 1 summarizes those conditions.

The three variables we have varied among the different simulation set are:

- The volumetric flow rate at the domain inlet and thus the bulk velocity. This quantity is expected to modify the thermocline degradation due to turbulent mixing
- The operation mode, which has been varied among charge, discharge and idle (i.e standby) periods
- The maximum and minimum temperature inside the tank

		T min[K]	T max [K]	Pe	Flow rate $\left[\frac{m^3}{s}\right]$	Bulk velocity [m/h]
Simulation 1	discharge	550	760	2,224	0.00107	1.241
Simulation 2	discharge	550	760	1,765	0.00085	0.985
Simulation 3	discharge	550	760	2,462	0.00013	0.146
Simulation 4	discharge	550	760	430	0.00021	0.242
Simulation 5	discharge	550	760	1,323	0.00063	0.738
Simulation 6	discharge	550	760	213	0.00010	0.119
Simulation 7	discharge	550	760	1,960	0.00094	1.094
Simulation 8	discharge	550	760	3,334	0.00160	1.861
Simulation 9	discharge	550	760	3,100	0.00149	1.730
Simulation 10	discharge	550	760	910	0.00044	0.508
Simulation 11	Idle	550	760	0	0.00000	0
Simulation 12	Idle	620	680	0	0.00000	0
Simulation 13	Idle	600	760	0	0.00000	0
Simulation 14	Charging	550	760	3,800	0.00182	2.121
Simulation 15	Charging	550	760	950	0.00046	0.530
Simulation 16	Charging	550	760	475	0.00023	0.265
Simulation 17	Charging	550	760	1,875	0.00029	0.339
Simulation 18	Charging	550	760	1,402	0.00022	0.253

Table 1. Simulation conditions

The initial temperature of the whole domain has been set equal to a step function, with salts at the maximum temperature in the upper part of the tank and cold salts at the bottom. This ideal thermocline is initially placed at $z = 0.3\ m$.

For each of the CFD simulations above the following variables are extracted for further elaboration:

- Fourier number at each time step obtained by calculating the weighted average thermal diffusivity on the vertical line. Averaging is necessary to produce a unique value of the Fourier number, which should be representative of the whole tank.
- Dimensionless temperature profile at each time step
- Peclet number at each time step obtained by calculating the weighted average thermal diffusivity on the vertical line. Averaging is again necessary to produce a unique value of Peclet number.

All these data are read in MATLAB where a fitting script has been built in order to determine the logistic distribution parameters for each time step of the simulation.

2.4 Second-law performance analysis

In a stratified thermal energy storage, the exergy concept is a bullet-point for the assessment of performances. In fact, the energy losses towards the environment are often negligible and the main thermodynamic losses are connected to second law irreversibilities.

Mixing is well-known to be a highly irreversible process [15] and, as such, it has to be properly accounted during the simulation of a molten salts storage tank. The concept of exergy is very useful in this case: the thermocline thickness increases and the entropy generation results in a reduction of the available work. Many parameters have been suggested in [16]. It is useful to compare the exergy content of a TES with two reference conditions: the fully mixed tank and the ideal tank while conserving the total energy of the tank. The former case applies when a sensible storage tank only has one single temperature level, as if the thermocline was infinitely thick. The latter case, on the other hand, corresponds to a nil thickness of the thermocline, which is the ideal situation from an exergetic point of view. Thermocline Exergetic Performance (TEP) is here proposed as the performance parameter to evaluate the storage systems performance. This is defined as:

$$TEP = \frac{Ex - Ex_{fm}}{Ex_{id} - Ex_{fm}} \tag{12}$$

For an ideal fluid with temperature gradients only in the z direction, the exergy can be written as:

$$Ex = \frac{\int_0^L \left(E + \rho\ c_p \mathrm{T}_0 \ln\left(\frac{T_0}{T(z)}\right)\right) dz}{L} \tag{13}$$

If the energy of the fluid is the same for the stratified, the fully mixed and the ideal thermal energy storage, the parameter TEP can be rewritten in the following way:

$$TEP = \frac{\int \ln\left(\frac{T_{fm}}{T}\right) dz}{\int \ln\left(\frac{T_{fm}}{T_{id}}\right) dz} \tag{14}$$

The stratified temperature T is a function of the non-dimensional z coordinate and this quantity should be integrated using the appropriate numerical technique. On the other hand, the two other temperatures can be defined in the following way:

$$T_{fm} = T_{mn} + \ (T_{mx} - T_{mn}) \frac{\int_0^1 T^* dz^*}{\int_0^1 dz^*} = T_{mn} + \ (T_{mx} - T_{mn}) \int_0^1 T^* dz^* \tag{15}$$

$$T_{id} = \begin{cases} T_{mn} & if\ z^* < zc_{id}^* \\ T_{mx} & if\ z^* > zc_{id}^* \end{cases} \tag{16}$$

The first integral can be obtained analytically. Using the variable substitution technique, we have:

$$\int_0^1 T^* dz^* = \left(1 + S \ln\left(\frac{1 + e^{\frac{zc^* - 1}{S}}}{1 + e^{\frac{zc^*}{S}}}\right)\right) \tag{17}$$

The coordinate zc_{id}^* is the non-dimensional thermocline position of the equivalent ideal temperature profile. This quantity can be calculated in a very straightforward way once the energy conservation condition is applied to obtain the equivalent temperature profile:

$$\int_0^1 T^* dz^* = T_{mn}^* zc_{id}^* + T_{mx}^* (1 - zc_{id}^*) \tag{18}$$

And knowing that $T_{mn}^* = 0$ and $T_{mx}^* = 1$ it is possible to obtain the simplified relation:

$$zc_{id}^* = 1 - \int_0^1 T^* dz^* \tag{19}$$

Figure 4 shows the calculated Thermocline Exergetic Performance for the case in which the minimum and maximum temperatures are set to 550 K and 770 K respectively. It is observed how the exergetic performance of the storage tank drops quickly in the first phase of the thermocline degradation and tends asymptotically to 0 for an infinitely large thermocline. Furthermore, the exergetic performance diminishes when the thermocline is not exactly placed in the center of the tank because the maximum temperature difference of the dimensionless profile becomes less than one and the vertical temperature profile gets more similar to the fully mixed one.

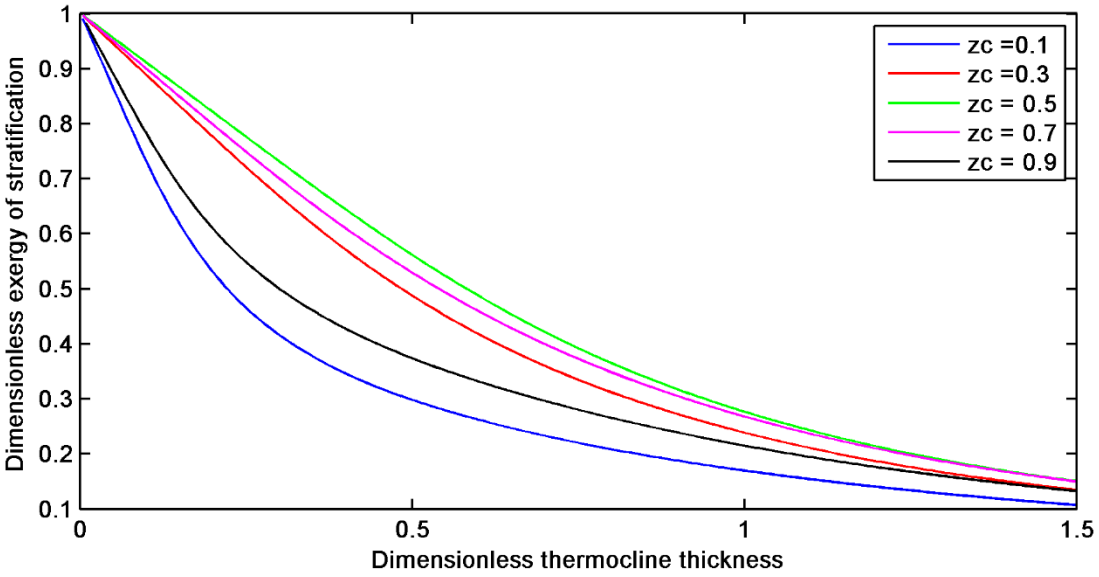

Figure 4. Thermocline Exergetic performance trend

2.5 Adaptation of the function for real power plant operation

The function derivation described in the previous section is based on many assumptions that are not always verified during the operation of real solar thermal power plants. In particular, it is worth mentioning three inconsistencies of the model compared to the real plant operation.

First of all, the temperature level of molten salts in the tank is not maintained constant during the discharging process. This is due in particular to the natural circulation in the submerged steam generator. On the other hand, the charging process is not a problem. In fact, the molten salts mass flow rate in the receiver tubes is normally varied in order to reach the highest allowable temperature. In order to tackle correctly the discharging inlet temperature variation, which could be quite relevant in natural circulation systems, an

energy conservation approach has been used. If the inlet temperature was maintained constant, the energy contained in the tank at a given time would be:

$$E_{ideal_i} = L\, A_{section} \bar{\rho} \bar{c}_p \left(T_{mn} + (T_{mx} - T_{mn}) \int_0^1 T_i^*\, dz^* \right) \tag{20}$$

However, during the time step $\Delta t_i = t_i - t_{i-1}$ a mass flow at a temperature different from T_{mn} is discharged. During the discharge process, the energy entering the domain during the time step Δt_i from the outlet of the steam generator, i.e. at the end of the Venturi Tube, is thus:

$$E_{disch_i} = \dot{V}_{disch} \Delta t_i\, \rho\, c_p T_{disch} = L_{disch} A_{section} \rho\, c_p T_{disch} \tag{21}$$

Hence, the real energy contained inside the tank at the time t_i can be written as follows:

$$E_{real_i} = E_{disch_i} + L\, A_{section} \bar{\rho} \bar{c}_p \left(T_{mn} + (T_{mx} - T_{mn}) \int_{\frac{L_{disch}}{L}}^1 T_i^*\, dz^* \right) \tag{22}$$

Where the second term is the ideal energy contained in the upper part of the tank which has not been substituted by the discharged volume. The real temperature profile can be written using the following conditions:

$$z^*_{c\,real} = z^*_{c\,ideal} \tag{23}$$

$$TC^*_{real} = TC^*_{ideal} \tag{24}$$

$$L\, A_{section} \bar{\rho} \bar{c}_p \left(T_{mn_{real}} + (T_{mx} - T_{mn_{real}}) \int_0^1 T_i^*\, dz^* \right) = E_{i\,real} \tag{25}$$

It is clear that a new value of the minimum temperature $T_{mn_{real}}$ inside the tank has to be chosen according with the energy conservation principle.

Secondly, the bulk velocity in the tank is not kept constant during a complete charge-discharge cycle as it changes frequently due to the mass flow rate variations described previously. This problem can be tackled with the differentiation of the equations proposed previously. The simulation can then be performed with a time integration of this differential equation. In mathematical terms:

$$z_c^*(Fo_i, Pe_i) = z_c^*(Fo_{i-1}) + Pe_i * Fo_i \quad (26)$$

$$TC^*(Fo_i, Re_i) = TC_{i-1}^* + \frac{\partial TC^*(Re_i, Fo_i)}{\partial Fo} * dFo \quad (27)$$

Thirdly, the Logistic distribution function is able to properly represent only situations in which the thermocline is contained entirely inside the tank. This is quite a strong approximation since it has been proved also in the framework of the present work, that the stratification degradation is quite visible and, after several hours, the thermocline would occupy the whole tank height. This situation results in the complete loss of thermal energy storage capacity. In fact, it is not possible to extract fluid from the tank at the desired temperature. Hence, the thermocline has to be partially or completely removed from the tank every once in a while. To analytically represent the situation, the approach proposed by Bayon et al. in [11] was followed. This consists in building an "apparent" dimensionless temperature profile that conserves the energy in the tank.

3 Results and discussion

The function proposed for the time evolution determination of the dimensionless thermocline thickness TC^* has the form:

$$TC^*(Re_{bulk}, Fo) = a\, Fo^{0.5} \quad (28)$$

$$a = f(Re_{bulk}) \quad (29)$$

In [7] and [8], it is suggested that the thermocline degradation should be proportional to $\sqrt{\alpha t}$, which is proportional to the Fourier number. The scale factor a was found to be a function of the bulk Reynolds number. In fact, the thermocline degradation is largely due to the fluid motion.

The scale factors obtained for the charging and discharging phases are plotted in Figure 5. The blue dots are the results of the discharge simulations. The scale factor a looks quite well aligned so that, for the range of Reynolds number considered, we can consider a linear relationship such as:

$$a = 11.907 + 0{,}0074\, Re_{bulk} \quad (30)$$

The charge simulations have shown a good agreement with the correlation found for the discharge. The results obtained in this case are plotted in the graph as a validation of the previous results obtained for the discharging phase.

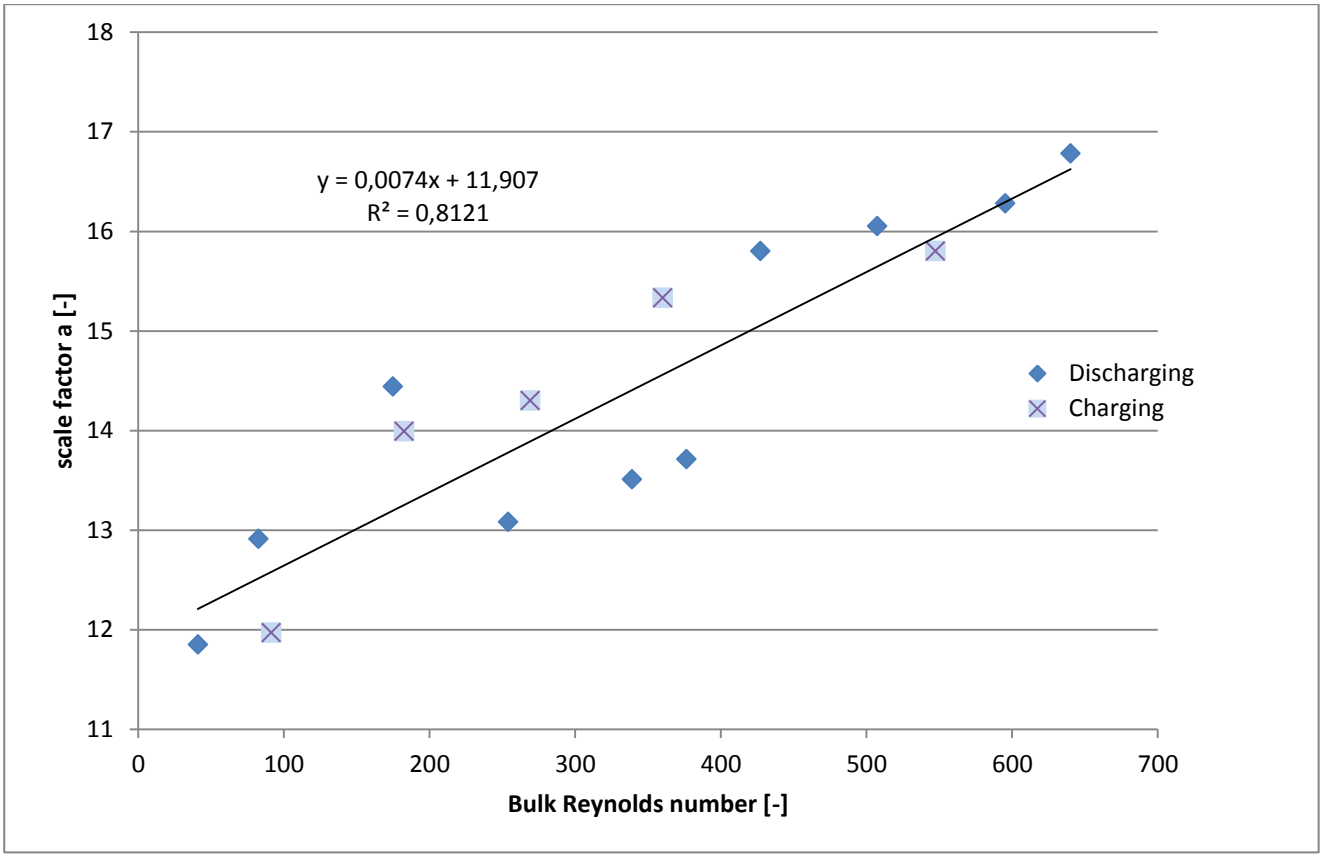

Figure 5. Scale factor dependence on Reynolds number

For idle periods, since the bulk velocity of the fluid should be set to 0 for the whole simulation, modifications of the simulation temperature levels were made in order to check the validity of the results obtained. In fact, if the initial conditions are the same, the temporal evolution of the S parameter and thus of the thermocline thickness should also be the same [8]. Table 2 shows the results obtained for three different cases.

delta T [°C]	**a**
210	11,78
60	11,12

160	11,27

Table 2. Simulations with different temperature levels

Even if it is possible that greater buoyancy induced currents result in greater mixing and expansion of the thermocline layers, differences among the three cases are very likely to be connected to purely numerical diffusion [18].

However, the results obtained show an increase of 6 % of the scale factor a if the temperature difference rises from 60 °C to 210 °C. Hence, the result obtained are considered good enough for the utilization of the function in year-round simulations. In conclusion, for standby periods we can write:

$$TC^* = 11.12\, Fo^{0.5}$$

4 Grid independence and adiabatic conditions

In order to test the suitability of the mesh chosen, a grid independence study has been conducted. The mesh element size in the z direction has been varied with equal-size step from 1 cm to 0.25 cm and the deviation of the scale factor $\boldsymbol{a}$ has been calculated. The results are given in Table 3. The element size in the radial direction is three times greater than the one in the axial direction.

It is observed that the mesh chosen for the multiple simulations, i.e. mesh 3, gives negligible deviation from the finer mesh. If the size of the element in the axial direction is increased slightly, however, the error increases dramatically up to around 18 %.

	Number of elements	**scale factor a**	**Deviation from mesh 4 [%]**
mesh 1: 1 cm	14,436	19.72	79.9
mesh 2: 0.75 cm	26,870	13.13	18.0
mesh 3:0.5 cm	41,331	11.12	1.4
mesh 4: 0.25 cm	119,405	10.96	0

Table 3. Grid independence study

A simulation in adiabatic condition has also been conducted for mesh 3 in order to quantify the effect of convective mixing due to heat losses towards the external environment. It is clear from the analysis of Table 4 that the mixing current due to free convective motion increases the rate of degradation of the thermocline

of roughly 7 %. However, this result is expected to be very different for a different choice of the tank insulation material and for different shape factor, i.e. the ratio of height to radius of the tank. The shape factor as well as the diffuser type at the inlet of the domain will also be crucial in the determination of the velocity field and thus of the entity of the turbulent mixing.

	Number of elements	scale factor a	Deviation from adiabatic conditions [%]
mesh 3 thermal losses	41,331	11.12	7.5
mesh 3 adiabatic	41,331	10.34	0

Table 4. Comparison with adiabatic conditions simulation

5 Validation

5.1 Comparison with CFD simulation results

As a validation of the proposed modeling approach, a CFD simulation has been performed varying the operation mode and the volumetric flow rate. The results obtained by the temporal integration of the analytic function are then compared to the CFD simulation results to check the accuracy.

Going more into details, the following inlet boundary conditions have been adopted for the CFD simulation:

$$DISCHARGING: \quad Q_{inlet}(t) = \left(80 - \frac{40}{3600}t\right) * 10^{-5} \left[\frac{m^3}{s}\right] \qquad for\ 0s < t < 3600s$$

$$IDLE: \quad Q_{inlet}(t) = 0 \left[\frac{m^3}{s}\right] \qquad for\ 3600s < t < 7200s$$

$$CHARGING: \quad Q_{inlet}(t) = \left(90 - \frac{50}{3600}t\right) * 10^{-5} \left[\frac{m^3}{s}\right] \qquad for\ 7200s < t < 10800s$$

To fully test the usability of the approach proposed, we have set initial and boundary conditions different from the cases simulated to parameterize the function (see Table 1). The initial temperature is set to 490 °C (fully charged condition of the tank), the cold salts are discharged at 280 °C while the hot salts are injected at 490 °C.

Referring to Figure 6, Figure 7 and Figure 8, the black dotted lines are obtained by the CFD simulation while the solid lines are the results of the integration of the analytic function. Each temperature profile is obtained every 900s. The results obtained by the temporal integration of the function show a nearly perfect agreement with the simulated ones except for a slight overestimated diffusion at the thermocline border. The values of the mean absolute error for the discharging, idle and charging phases are calculated to be 0.47 K, 1.81K and 2.28 K with error standard deviations of 0.68 K, 2.20 K and 2.91 K respectively.

It should be noticed that the time step utilized for the integration should be quite small for a good accuracy. The results shown here are obtained with a time-step of 60 seconds and by far worse results were obtained integrating every 300 s and 180 s.

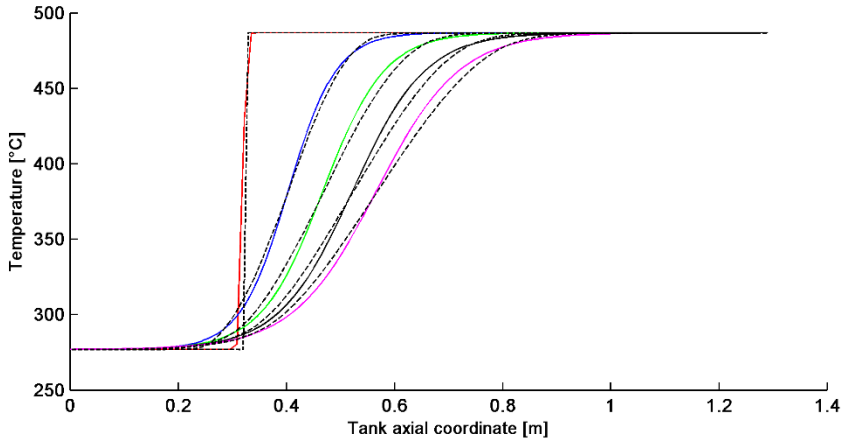

Figure 6. Discharging. The front is moving from left to right. Curves are calculated from 0 s to 3600 s every 900 s

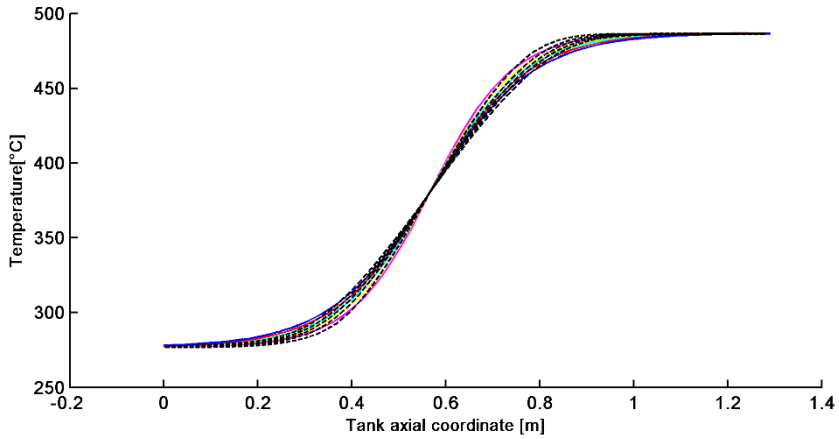

Figure 7. Idle period. The thermocline thickness is increasing from 3600 s to 7200 s with time steps of 900 s

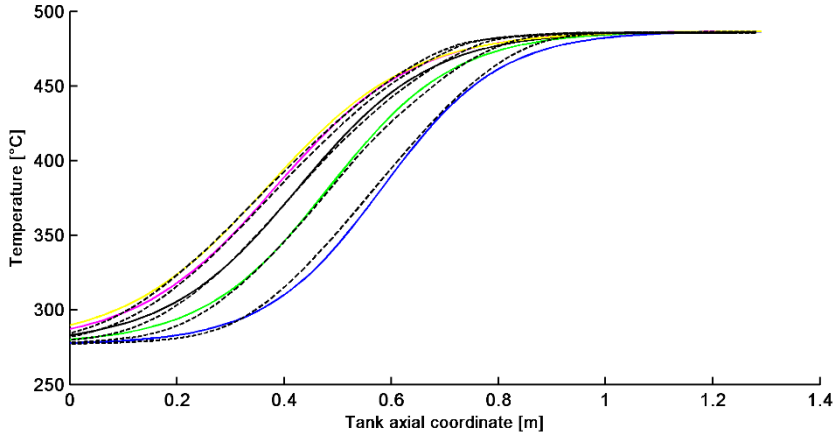

Figure 8. Charging. The front is moving from right to left. Calculated curves are from 7200 s to 10800 s with time steps of 900 s

5.2 Comparison with literature data

Chung [8], in his integral approximation of the charging process, proposed to represent the dimensionless temperature profile with a Fermi-Dirac distribution and found, after some simplifications, that the thermocline thickness, defined in the same way as the present work, can be considered independent from the Peclet number and can be described by:

$$TC^* = 2\sqrt{24Fo} = 9.79\sqrt{Fo} \qquad (32)$$

After some elaboration of the data obtained by the numerical approach followed by Bayon and Roya [11], their relation for the dimensionless thermocline thickness during idle periods was found to be:

$$TC^* = 10.99\sqrt{Fo} \qquad (33)$$

These results should be compared with the ones obtained in the framework of the present work for standby periods, since it was showed that the fluid velocity is modifying the thermocline due to turbulent mixing and buoyancy induced currents. Also all the models presented are solving the problem in completely adiabatic conditions. The scale factor we obtained in the same conditions is equal to 10.34. The deviation of the present work compared to the previous ones is thus in the order of -5 % with respect to [11] and +6 % with respect to [8]. Many factors could contribute to this deviation but numerical diffusion is certainly very likely. In fact, the results are very similar to the work proposed by Roja and Bayon [11] that also used a numerical technique which is certainly affected by the choice of the number of nodes. It has been shown in [19], however, that a bad grid choice can deeply affect the results in the short term, i.e. single charge-discharge cycle, but results obtained for long term simulations are far less sensitive to the number of nodes used .

The results obtained here are believed to be a valuable prediction tool for every stratified thermal energy storage tank. For instance, the work of Verda and Colella [20] for a district heating water storage tank is used here as a comparison. In that work, the authors modeled the turbulent charging and discharging process with a laminar mono-dimensional finite difference scheme where the thermal conductivity of water was calibrated in order to fit the results of some CFD turbulent simulations performed with FLUENT. The velocities involved in their work are much greater than the ones we modeled and the flow pattern is fully turbulent along the whole tank height, while normally in molten salts storage tank for CSP applications the velocity is slow in order to keep the turbulent mixing as limited as possible. However, we have demonstrated that some mixing phenomena are still present and can be directly linked to the bulk velocity.

The comparison between the temperature profiles they obtained for the case at half of the full power (where the loss of thermal stratification is more visible) and the ones obtained with the present approach by setting the water thermal conductivity $k_{water}$to $600\,\frac{W}{mK}$, as they have proposed to take into consideration turbulent effects, is graphically shown in Figure 9. The temperature profiles obtained in [20] are here rebuilt using the logistic function and using the thermocline thickness obtained by the elaboration of their work. On the other hand, the correlation here used for the scale factor a is the one obtained for standby periods because the effect of turbulences is already accounted with the value of k_{water} and its value for such a high Reynolds number was not verified.

The good agreement obtained shows that the function is able to represent a wide variety of processes that involve the thermal stratification of a fluid.

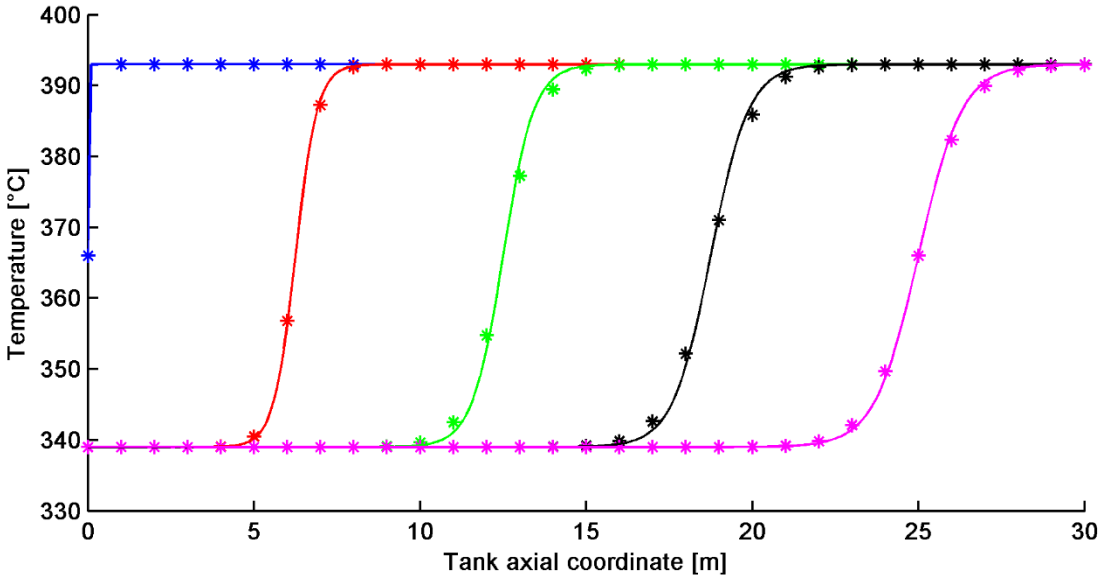

Figure 9. Comparison of results with a district heating storage tank discharging. Starred points belong to Verda et al. while solid lines are obtained with the function proposed. Different colors are referred to different times, blue is 0s, red is 1150 s, green is 2300s, black is 3450 s and magenta is 4600s

6 Conclusions

This paper presents a methodology for the adaptation of a storage tank CFD model for system-level simulations and optimizations. An analytical function, namely the logistic cumulative distribution, was considered because it is able to represent the trend of the temperature profile along the axial coordinate for charging, discharging and standby periods under different conditions. Eighteen CFD simulations were performed in order to statistically parameterize the function under variable conditions.

The proposed approach has demonstrated to be successful in reproducing the results of CFD simulations, even with variable mass flow and variable inlet temperature conditions. This means that the detailed features are preserved, but time required for solution is dramatically reduced. Furthermore, it has the advantage of being independent on the value chosen for the maximum and minimum temperature in the tank, which makes it usable for a wide range of processes and systems, from low-temperature storage in district heating to high-

temperature storage in Concentrated Solar Power. The model can be efficiently applied to the design/operation optimization of complex systems operating in transient mode. Such analysis, in fact, requires to adopt models that capture the behavior caused by variation in the design and operation variables but sufficiently compact to allow their application within iterative algorithms containing simulations of long operation periods.

Acknowledgements

The research leading the results reported in this paper has received funding from the European Union's Seventh Framework Program (FP7/2007-2013) under grant agreement n. 268219 for MATS project (Multipurpose Applications by Thermodynamic Solar).

References

[1] W. Gaggioli and L. Rinaldi, "An Innovative Concept of a Thermal Energy Storage (TES) System Based on the Single Tank Configuration Using Stratifying Molten Salts (MS) as both HSM and HTF, and with an Integrated Steam," in *SolarPACES international Conference 2013*, 2014, pp. 780–789.

[2] IRENA, "Concentrating Solar Power," Abu Dabhi, UAE, Renewable Energy Technologies: Cost analysis series,Volume 1: power sector, 2012.

[3] W. Yaïci, M. Ghorab, E. Entchev, and S. Hayden, "Three-dimensional unsteady CFD simulations of a thermal storage tank performance for optimum design," *Appl. Therm. Eng.*, vol. 60, no. 1–2, pp. 152–163, Oct. 2013.

[4] E. Rivas, E. Rojas, R. Bayón, W. Gaggioli, L. Rinaldi, and F. Fabrizi, "CFD Model of a Molten Salt Tank with Integrated Steam Generator," *Energy Procedia*, vol. 49, pp. 956–964, 2014.

[5] S. a. Zavattoni, M. C. Barbato, a. Pedretti, G. Zanganeh, and a. Steinfeld, "High Temperature Rock-bed TES System Suitable for Industrial-scale CSP Plant – CFD Analysis Under Charge/Discharge Cyclic Conditions," *Energy Procedia*, vol. 46, pp. 124–133, 2014.

[6] E. Pak, "Theoretical model of the charging process for stratified thermal storage tanks," *Sol. Energy*, vol. 51, no. 6, pp. 513–519, 1993.

[7] E.R.G. Eckert, R.M. Drake, *Analysis of Heat and Mass Transfer*, McGraw Hill, New York, NJ, 1972

[8] J. D. Chung and Y. Shin, "Integral approximate solution for the charging process in stratified thermal storage tanks," *Sol. Energy*, vol. 85, no. 11, pp. 3010–3016, Nov. 2011.

[9] G. J. Kolb, "Evaluation of Annual Performance of 2-Tank and Thermocline Thermal Storage Systems for Trough Plants," *J. Sol. Energy Eng.*, vol. 133, no. 3, p. 031023, 2011.

[10] G. Angrisani, M. Canelli, C. Roselli, M. Sasso, "Calibration and validation of a thermal Energy Storage model: Influence on simulation results," *Appl. Therm. Eng.*, vol. 67, pp. 190–200, 2014

[11] R. Bayón and E. Rojas, "Analytical function describing the behaviour of a thermocline storage tank : A requirement for annual simulations of solar thermal power plants," *Int. J. Heat Mass Transf.*, vol. 68, pp. 641–648, 2014.

[12] B. Adrian, *Advanced Engineering Thermodynamics*, John Wiley, New York, NJ, 2006.

[13] K. Lichtenegger and B. Hebenstreit, *Model for stratified thermal storage tank*, Master Thesis, Politecnico di Milano, Italy, 2013.

[14] J. Waluyo, "Performance evaluation of stratified TES using Sigmoid Dose Response Function," *J. Appl. Sci.*, vol. 11, no. 9, pp. 1642–1647, 2011.

[15] N. H. Moran, J. Michael, Shapiro, *Fundamentals of Engineering Thermodynamics*, John Wiley & Sons, New York, NJ, 2010.

[16] M. a Rosen, "The exergy of stratified thermal energy storages," *Sol. Energy*, vol. 71, no. 3, pp. 173–185, Jan. 2001.

[17] K. M. Powell and T. F. Edgar, "An adaptive-grid model for dynamic simulation of thermocline thermal energy storage systems," *Energy Convers. Manag.*, vol. 76, pp. 865–873, Dec. 2013.

[18] A. Younes, M. Fahs, and P. Ackerer, "A new approach to avoid excessive numerical diffusion in Eulerian – Lagrangian methods," *Commun. Numer. methods engeneering*, vol. 24, no. March 2007, pp. 897–910, 2008.

[19] D. A. Arias, A. C. Mcmahan, and S. A. Klein, "Sensitivity of long-term performance simulations of solar energy systems to the degree of stratification in the thermal storage unit," *Int. J. Energy Res.*, vol. 32, no. December 2006, pp. 242–254, 2008.

[20] V. Verda and F. Colella, "Primary energy savings through thermal storage in district heating networks," *Energy*, vol. 36, no. 7, pp. 4278–4286, Jul. 2011.